Geophysical Research Letters

RESEARCH LETTER
10.1029/2018GL077760

Special Section:
Impact of the Sept. 10, 2017, solar event on Mars

Analysis of the Radiation Hazard Observed by RAD on the Surface of Mars During the September 2017 Solar Particle Event

C. Zeitlin[1], D. M. Hassler[2], J. Guo[3], B. Ehresmann[2], R. F. Wimmer-Schweingruber[3], S. C. R. Rafkin[2], J. L. Freiherr von Forstner[3], H. Lohf[3], T. Berger[4], D. Matthiae[4], and G. Reitz[4]

[1]Leidos Innovations Corporation, Houston, TX, USA, [2]Southwest Research Institute, Boulder, CO, USA, [3]Department of Physics, Christian Albrechts University, Kiel, Germany, [4]German Aerospace Center, Cologne, Germany

Abstract We report dosimetric quantities measured by the Mars Science Laboratory Radiation Assessment Detector (RAD) on the surface of Mars during the 10–12 September 2017 solar particle event. Despite 23 g/cm^2 of CO_2 shielding provided by the atmosphere above RAD, dose rates rose above background galactic cosmic ray levels by factors of 2 to 3 over the course of several hours and leveled off at sustained peak rates for about 12 hr before declining over the following 36 hr. As the solar particle event flux was gradually declining, a shock front reached Mars and caused a sudden drop of about 15% in instantaneous dose rates. No solar particles followed the shock arrival, and the magnetic shielding of galactic cosmic rays by the shock reduced their intensity to levels below those seen before the start of the event. This event is the largest seen to date by RAD on Mars.

Plain Language Summary We report the radiation dose rate on the surface of Mars measured by the Radiation Assessment Detector (RAD) aboard the Curiosity rover before, during, and after the solar energetic particle (SEP) event of 10–12 September 2017. Future astronauts exploring Mars will be at risk from SEP events, which occur sporadically and often with little warning, as well as from galactic cosmic rays, which are a continuous source of radiation dose and which generally have higher energies than SEPs. The event described here was the largest so far observed by RAD in more than five years on Mars. Although the atmosphere of Mars is only about 1–2% as thick as Earth's, it provides a measure of shielding against solar particles, most of which are protons with energies insufficient to penetrate Mars' atmosphere and reach the surface. But in this event, RAD saw a clear increase in dose rates; the peak dose rate was nearly three times above galactic cosmic ray levels measured prior to the event. Though the increase was rapid and lasted for three days, it was too small to represent a risk to the health of an astronaut receiving it. Much larger SEP events are possible and could cause problematic doses.

Key Points:
- Protons accelerated during the large solar particle event of September 2017 reached the surface of Mars and were observed by MSL-RAD
- Dose rates were seen to increase by factors of 2 to 3 above the background level of the galactic cosmic rays
- Doses integrated over a 30-day interval that included the event remained well below NASA radiation exposure limits for astronauts

Correspondence to:
C. Zeitlin,
cary.j.zeitlin@nasa.gov

Citation:
Zeitlin, C., Hassler, D. M., Guo, J., Ehresmann, B., Wimmer-Schweingruber, R. F., Rafkin, S. C. R., et al. (2018). Analysis of the radiation hazard observed by RAD on the surface of Mars during the September 2017 solar particle event. *Geophysical Research Letters*, *45*, 5845–5851. https://doi.org/10.1029/2018GL077760

Received 2 MAR 2018
Accepted 9 MAY 2018
Accepted article online 18 MAY 2018
Published online 29 JUN 2018

1. Introduction

Solar activity became surprisingly intense in September 2017, due to Active Region 2673, which produced four X-class flares between 4 and 10 September. Enhancements were seen in various GOES proton channels (Onsager et al., 1996); prior to 10 September, enhancements were seen only in channels that measure protons with kinetic energies below 100 MeV, with the exception of a small, brief rise in the >100 MeV channel on 6 September. However, following the 10 September flare, GOES observed a large, rapidly rising spike in the >100 MeV proton flux. This channel is important when considering shielded environments such as the interior of a spacecraft in interplanetary space and the Martian surface, because such energetic protons can penetrate modest depths of shielding and can potentially impart dangerous doses to astronauts. When Earth and Mars are widely separated in terms of heliospheric longitude, as was the case in September 2017 (approximately 155° separation), an event seen at one planet might not be seen at the other. This event was seen on both planets, and by several instruments aboard the International Space Station. Kinematics and modeling of the coronal mass ejections that produced the particle event are described elsewhere (Guo et al., 2018).

2. Triggering and Data Acquisition

The Radiation Assessment Detector aboard the Mars Science Laboratory (MSL-RAD) has been described in the literature (Hassler et al., 2012; Zeitlin et al., 2016). Dosimetric results (Guo et al., 2015; Hassler et al., 2014; Zeitlin et al., 2013) have also been reported. Figure 1 shows a schematic diagram of the detectors

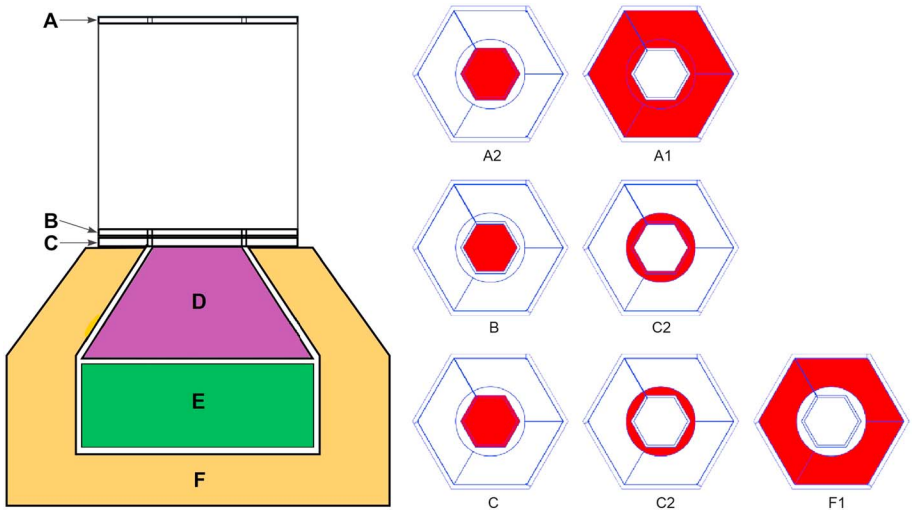

Figure 1. Schematic drawing of the RAD sensor head, left, showing the stack consisting of three silicon detectors (A, B, and C) and three scintillators (D, E, and F). The scintillators enable measurements of neutral particle spectra and are also useful for charged particle measurements. The segmentation of the silicon diodes is as indicated on the right; light from the F scintillator is collected in the outermost segments of the C detector diode.

contained in the sensor head. The A silicon detector is roughly level with the rover's deck, and the detector generally points within a few degrees of vertical. RAD records dose rate information in real time in its onboard data processing using the B (silicon) and E (plastic) detectors. The dosimetry triggers (one for B, one for E) accept any energy deposition above threshold in either detector; running sums are kept onboard for telemetry to Earth. Because each of these triggers depends only on a single detector, there are no restrictions on the direction of incidence of incoming particles; that is, these triggers enable dose measurements with omnidirectional detector responses. RAD also has triggers for incident energetic charged particles, which require coincidences of the A and B silicon detectors, which are the topmost two detectors in the stack. The A detector consists of outer (A1) and inner (A2) segments. Unlike the omnidirectional responses of the dosimetry triggers, these viewing cones are restricted: A2*B coincidences occur when charged particles arrive at angles less than about 18° from the vertical, and A1*B coincidences occur for incident angles from about 18° to 30°. When either trigger fires, all hit detectors are read out, and the complete event record is stored, provided storage space is available. If storage is unavailable, the event is counted, enabling needed corrections in subsequent data analysis.

RAD also has counters that group triggered events into broad categories. Of interest here are the counters for vertical penetrating charged particles (defined as simultaneous hits in the A2, B, C, D, E, and F2 detectors) and for vertical charged particles that stop in the D detector (hits in A2, B, C, and D only). Counters are also defined for neutral particles in the D and E detectors.

RAD runs on an autonomous observing cadence, set to 16 min in solar quiet time but switching to 8 min when high count rates are observed during the 10-s sampling period prior to the start of each observation. At the end of each measurement period, data are stored internally for later telemetry to Earth.

In the following, the dose rates recorded by the B silicon detector have been converted, approximately, to dose rates in water, which is the quantity of interest for radiation dosimetry. A constant scaling factor of 1.3 has been applied to the silicon dose rate data. No conversion is applied to the data from the E detector, as plastic is close to water in terms of its response to the energetic charged particles that dominate the radiation environment on Mars.

3. Results

3.1. Event Timeline

Figure 2a shows the dose rates as recorded in the B and E detectors from 12:00 UTC on 9 September through midnight UTC of 15 September. Prior to the onset of the event, dose rates in RAD were entirely due to galactic

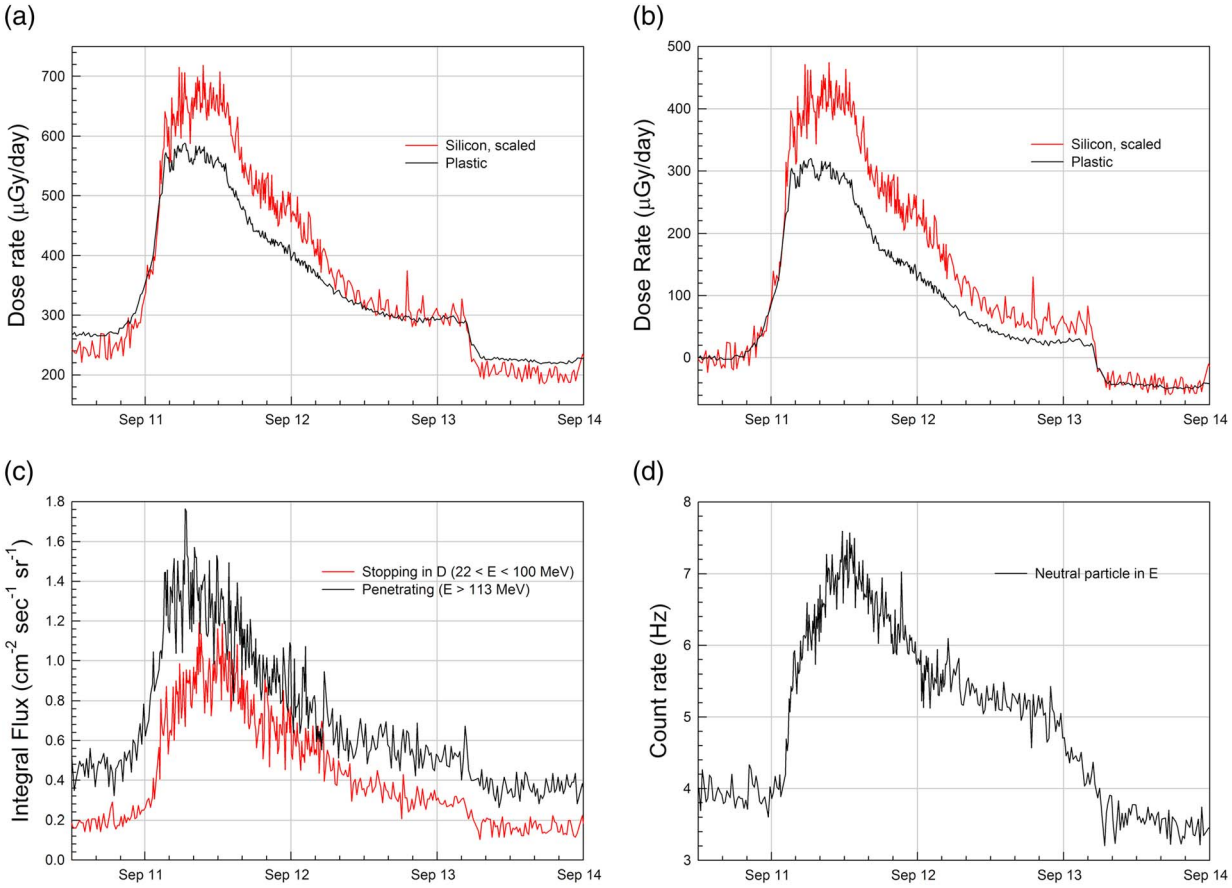

Figure 2. Dose rates as measured on Mars using the "B" silicon detector and "E" plastic scintillator. (a) Dose rates include contributions from galactic cosmic rays. (b) These contributions are subtracted. (c) The integral fluxes of stopping and penetrating particles seen before, during, and after the event. (Quoted energy ranges are for protons.) (d) The count rate of neutral particles hitting the E detector in the same time period.

cosmic rays (GCRs). The B dose rate averaged over 8 and 9 September was 244 μGy/day in water (after conversion from silicon), and the E dose rate averaged 268 μGy/day in plastic for the same days. The ~10% difference in dose rates is expected based on the different responses of the detectors to energetic charged particles; there is also a small contribution to the E dose rate from high-energy neutrons ($E > 6$ MeV), on the order of a few percent of the total during solar quiet time (Köhler et al., 2014).

Figure 2b shows the same dose rate data as Figure 2a, but with the average pre-SPE GCR dose rates subtracted. During the event, the dose rate in the B detector exceeded that in E because E is shielded by the surrounding detectors, and low-energy solar particles that deposit energy in B stop before they reach E.

A steady, statistically significant increase in the E dose rate started around 19:50 UTC on 10 September. By 03:00 UTC on 11 September, both B and E dose rates had reached about 90% of the eventual peak dose rates, which came a few hours later at about 07:00. There is considerable structure in the dose rates, particularly in the B detector data, though it is nosier statistically than E due to its smaller volume.

The event peaked on 11 September, from about 4:00 to 14:00 UTC. Dose rates then fell gradually until about 05:00 UTC on 13 September, at which point they fell steeply (see Figure 1b). Following the steep fall, associated with the arrival of the shock front of the interplanetary coronal mass ejection at Mars, no evidence of solar particles was observed, and GCR rates dropped to a (highly significant) level 15–20% below the rates prior to the event. Propagation of the shock through interplanetary space is discussed by Guo et al. (2018).

In the declining phase of the SPE, the dose rate in the B detector stayed at higher rates longer than that in the E detector, reflecting the typical softening of SPE spectra seen during prolonged events. Integrating the B and

E dose rates for the period from the start of the event until the arrival of the shock front at Mars, we find that the SPE contributed 544 μGy of dose in water as measured by the B detector, and 369 μGy of dose as measured by E. These are the estimated doses above GCR that are attributable to the SPE.

The fact that the dose rates in both B and E climbed by roughly similar amounts is notable. For particles coming into RAD from above, B is shielded by the atmosphere, which had an average vertical column depth 23.4 g/cm^2 during this period. This stops protons with kinetic energies less than about 175 MeV. The B detector is additionally shielded by two very thin windows and the A detector, but these are negligible for present purposes. The E detector is shielded by the same things, plus the B, C, and—most importantly—D detectors, the latter consisting of 12.54 g/cm^2 of CsI. Vertical protons energetic enough to reach RAD will stop in D (or higher up in the stack) if their remaining energy is less than 100 MeV. Thus, any proton—or ^{4}He ion—that reaches E and deposits energy there must have had a kinetic energy of at least 275 MeV/nuc at the top of the Martian atmosphere, whereas the corresponding minimum energy to deposit energy in B is 175 MeV/nuc. This difference in minimum energy explains the higher dose rate observed in B during the SPE. It is also clear that the event had a hard spectrum, a conclusion further supported by the spectral analysis presented elsewhere in this issue and by the fact that a ground-level enhancement was also seen at Earth starting at about 16:15 UTC on 10 September. (Neutron-monitor data for ground-level enhancements, including this one—number 72—can be found at http://www.nmdb.edu.)

The coincidence count rates for vertical charged particles that either stop in D or penetrate the entire detector stack are also of interest. Protons in the former category have kinetic energies in the range from 24 to 100 MeV when they enter RAD, and protons in the latter category must have at least 113 MeV when they enter RAD. (Incident protons with energies below 24 MeV either do not reach D or do not deposit sufficient energy to fire the D discriminator; protons with energies from 100 to 113 MeV stop in E.) Figure 2c shows the fluxes derived from these two count rates. It is important to note that the stopping flux shown here includes a large contribution from secondary electrons with energies in the 8 to 85 MeV range, which account for about 75% of the total. The flux of penetrating particles started increasing before the stopping flux did, reflecting the earlier arrival times of more energetic ions. The penetrating flux eventually rose by a factor of 3 compared to the period just before the SPE. The stopping flux increased by about a factor of 5 compared to quiet time, but more detailed analysis that excludes the electron contribution shows that the flux of stopping protons increased by about a factor of 30 compared to quiet time.

The increased flux of charged particles also produced an increased flux of neutral particles. Figure 2d shows the corrected count rate of hits in the E detector with no simultaneous hits in the other detectors that comprise the anticoincidence system. The E detector is sensitive to neutrons with energies above about 8 MeV, and, to a lesser extent, γ rays. The increase in flux relative to solar quiet time is less than a factor of 2. The increase of the neutral count rate appears to have been delayed by several hours relative to the arrival of charged particles. The cause of the delay is not obvious and is the subject of ongoing investigation.

The onset time of the event is an important consideration for future human explorers who would likely perform expeditions in which they drive considerable distances from their habitat. The event as seen on Mars was unambiguously underway by about 21:00 UTC on 10 September, and dose rates doubled within about 7 hr. If one were relying only on monitors on the surface of Mars or in orbit, this could be problematic for long drives, particularly in the case of a more intense solar event. However, for this event, the exposure incurred by being away from shelter for the duration would have been comparable to adding about two days of GCR exposure. In the context of a long-stay mission scenario, with a surface mission on the order of hundreds of days, this is insignificant. The Forbush decrease (FD) that followed the event mitigated even this small increase.

3.2. Deposited Energy Spectra and Radiation Quality Factors for Vertical Ions

It has long been known that the biological damage caused by radiation does not depend simply on physical dose, which is the energy deposited per unit mass (Rossi, 1964). This fact has motivated the use of radiation quality factors, which are particularly important in the context of human spaceflight. This is because the GCRs include high-energy heavy ions, the biological effects of which are known to be—for some biological endpoints—very large per unit dose compared to more common radiation types such as γ rays or X-rays (Blakely & Kronenberg, 1998).

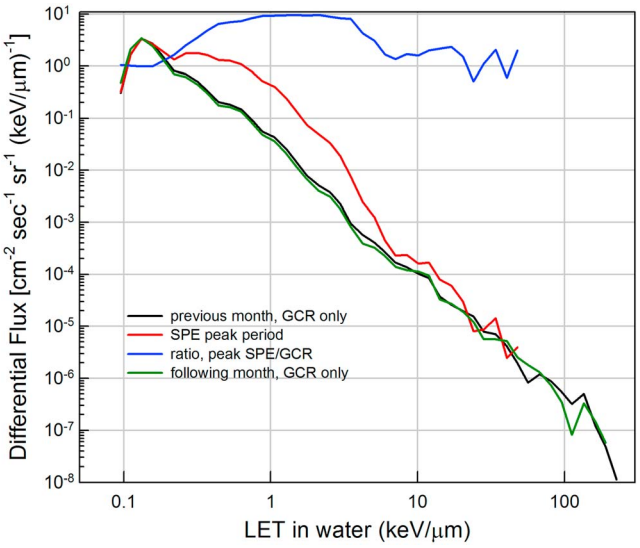

Figure 3. Differential LET spectra measured by MSL-RAD on Mars for 30 days prior to the event (black curve), 30 days after the event (green curve), and during the SPE peak (red curve). Spectra in water are obtained by scaling spectra measured in the B silicon detector. Measured particles are incident vertically on RAD. Also shown (blue curve) is the ratio of the event-peak flux to the quiet time GCR flux, showing that the flux increase was greatest below 10 keV/μm.

Here we use the quality factor defined by International Commission on Radiation Protection (ICRP) Report 60 (International Commission on Radiation Protection, 1991). Calculation of the dose equivalent, written as *H*, depends on knowledge of the dose and linear energy transfer (LET) spectrum in water. RAD measures LET in silicon for particles in either of the A*B coincidence cones (i.e., for incident angles <30° from the vertical). We perform an approximate conversion from the measured dE/dx in silicon to LET in using a simple scaling factor. The conversion factor is, in principle, energy-dependent, and for thin detectors such as the silicon detectors in RAD, should take account of losses due to escaping "knock-on" electrons. A reasonable estimate of the factor is 1.79; that is, LET in silicon is divided by this factor to obtain the approximate corresponding LET in water (which yields the dose conversion factor of 1.30 used in the preceding). The ICRP 60 report defines Q(LET), or Q(L), as a piecewise function with a value of 1.0 for LETs below 10 keV/μm, the range populated by the large majority of the observed SEPs.

Although GCR dose rates dropped by 15–20% immediately after the end of the event at Mars, there is no indication of GCR suppression during the event; we therefore use data taken prior to the onset of the event to estimate the GCR spectrum during the event. High-LET events are rare, so a comparatively lengthy period of 30 days was chosen, and similarly for the period after the event. Even with 30-day integration times, statistics at high LET are meager. The spectrum for the period before the event is shown as the black curve in Figure 3, the spectrum obtained during the peak of the event is shown in red, and the ratio of the two is shown in blue. The spectrum obtained from the 30 days following the event is shown in green; it is nearly indistinguishable from the preevent spectrum.

The peak of the SPE was (somewhat arbitrarily) defined as the time period during which the dose rate in E exceeded 100 μGy/day after subtracting the GCR background. This period runs from 1:23 UTC on 11 September until 3:16 UTC on 12 September, during which the flux of minimum-ionizing singly charged particles was virtually unchanged compared to the GCR spectrum for the prior month. This peak appears at LET of about 0.14 keV/μm, consistent with the calculated most probable energy deposit for minimum-ionizing protons in 300 μm of silicon (Bichsel, 1988) when our factor for scaling to water is applied. This value of LET is not the same as the mean LET in water (0.20 keV/μm) from the Bethe formula (Patrignani & Particle Data Group, 2016) for minimum-ionizing protons; the difference is due to straggling.

At LET values above about 0.18 keV/μm—corresponding to most probable energy depositions of protons with energies below about 800 MeV—the flux during the event was enhanced compared to quiet time levels. The enhancement reached a factor of nearly 10 in the LET range from about 1.5 keV/μm to 2.1 keV/μm. In this range, there may be a contribution from energetic helium ions, but if so, it is not distinguishable on the basis of LET alone. Between about 6 and 20 keV/μm, the flux enhancement is modest—the ratio averages less than 2 in this region. Above 20 keV/μm, the spectrum during the event is consistent, within statistics, with being purely GCRs. In this brief interval of maximum flux intensity, no events were seen with LET above 50 keV/μm.

The LET spectra have been integrated against the ICRP 60 Q(L) to obtain average radiation quality factor <Q> and dose equivalent for each period. Events in the A2*B field of view were used to obtain the <Q> values. For the most intense portion of the SPE, <Q> was 1.17, compared to values of 2.3 found for GCR-only periods before and after the event. The GCR <Q> of 2.3 is less than our previously reported value of 3.0 from early in the mission (Hassler et al., 2014), owing primarily to seasonal variations in the atmospheric column depth.

Table 1 shows rates for both the B and E detectors using the omnidirectional dose data as described above. The B dose rates have been converted to water using the 1.30 factor mentioned above. The dose equivalent rate in B is also shown (obtained by multiplying the dose rate by the appropriate <Q> for the time period). Despite the significant dose rate increase during the event, the peak dose equivalent rate in the B detector—which can be considered to be something like a skin exposure—was only about 50% greater than the GCR

Table 1
Dose and Dose Equivalent Rates and Totals

	Average rates 5-day pre-SPE	Peak rates during SPE	Average rates during SPE	Average rates 5-day post-SPE	Totals, 30 days before SPE	Totals,30 days starting 11/9/17
B, omnidirectional	240 μGy/day	718 μGy/day	464 μGy/day	208 μGy/day	7.3 mGy	7.7 mGy
E, omnidirectional	265 μGy/day	588 μGy/day	417 μGy/day	232 μGy/day	8.1 mGy	8.2 mGy
Dose equivalent using B	543 μSv/day	841 μSv/day	543 μSv/day	480 μSv/day	16.5 mSv	16.6 mSv

dose equivalent rates before and after the event, and the average dose equivalent rate during the event was nearly identical to GCR rates before. The FD that immediately followed the event caused GCR dose rates in both B and E to drop by 12% in the 5-day period after the event. GCR rates then recovered gradually, and by mid-October had returned to the levels seen before the event.

We have investigated the effect of the event on the integrated dose and dose equivalent the 30 days prior to the start of the event, and for the 30-day period that starts with the onset of the event as seen on Mars. Results are shown in the two right-most columns of Table 1. The FD that followed the arrival of the interplanetary coronal mass ejection shock at Mars caused GCR dose rates to drop by about 5% when averaged over this longer period (compared to the ~12% decreases in the five days immediately afterward). Considered over these two 30-day periods, the effect of the FD almost exactly offset the dose and dose equivalent contributions of the SPE in both B and E detector data. Note that the effective $<Q>$ for the 30-day period including the event is 2.15, slightly less than the GCR $<Q>$ due to dilution by the predominantly low-LET particles in the SPE. For all practical purposes, there is no difference in the accumulated exposures in the two periods.

One cannot generalize from this event to other SPE scenarios. Mars was not magnetically connected to the acceleration site until a later phase (Guo et al., 2018); had the active region been better connected to Mars, the dose rate increases would likely have been much larger. Also, the atmospheric shielding above RAD—23 g/cm^2 during the event—is greater than at higher elevations on Mars. At the mean Martian elevation, the vertical column depth of atmosphere is 16 g/cm^2, and—depending on the energy spectrum of the SEPs—there can be considerably larger exposures at this (and higher) elevation.

In the assessment of deterministic (noncancer) effects of radiation, the unit of gray equivalent (Gy-Eq) is used to account for the enhanced biological effectiveness of protons compared to photons. A relative biological effectiveness factor of 1.5 is assigned to protons in National Council on Radiation Protection and Measurements Report 142 (National Council on Radiation Protection and Measurements, 2002). National Council on Radiation Protection and Measurements has also defined 30-day exposure limits for astronauts (National Council on Radiation Protection and Measurements, 1989). Multiplying the SPE doses quoted above (544 μGy in B and 369 μGy in the more-shielded E detector) by the proton relative biological effectiveness of 1.5 yields exposures far below even the smallest of the 30-day exposure limits, which is 250 mGy-Eq for the heart and blood-forming organs. Even if the event had been an order of magnitude more intense, there would have been a large safety margin.

4. Conclusions

The SPE of September 2017 accelerated particles to energies high enough to easily penetrate the Martian atmosphere, even in Gale Crater, more than 4 km below the mean elevation on Mars. MSL-RAD observed roughly factor-of-two increases in dose rates, both in the lightly shielded B detector and in the more-shielded E detector. The count rate of neutral particles in the E detector, dominantly low-energy neutrons, rose by a factor of about 2 during the event, while the counts of penetrating ($E_{proton} > 113$ MeV) and stopping particles rose by factors of 3 and 5, respectively. Folding the LET spectrum of vertical-going particles with the ICRP 60 quality factor yields an average quality factor $<Q>$ of 1.17 during the peak of the event, compared to values of about 2.3 found for GCR-only spectra before and after the event. For purposes of calculating dose equivalent, the decrease in $<Q>$ tends to offset the increase in dose rates, so that the dose equivalent rate was only slightly greater than during the preceding solar quiet time in the B detector and was actually slightly below the quiet time rate in the E detector. The FD following the event reduced GCR dose rates, yielding integrated doses and dose equivalents for the 30-day period including the event that are only slightly greater than for

the 30-day period prior to the event. These exposures are well below National Aeronautics and Space Administration's 30-day limits. However, it is not possible to generalize from one medium-size event to other SPE scenarios. Mars was not magnetically connected to the active region on the Sun at the time of the 10 September flare; a well-connected event with the same hard spectrum would certainly produce much larger dose rates on the Martian surface and would likely produce a stronger FD following the SPE.

Acknowledgments
This work was supported by the NASA Johnson Space Center through NASA Human Health and Performance Contract NNJ15HK11B. The MSL-RAD project is supported in the United States by the National Aeronautics and Space Administration's Human Exploration and Operations Mission Directorate, under Jet Propulsion Laboratory subcontract 1273039 to Southwest Research Institute, and in Germany by the German Aerospace Center (DLR) and DLR's Space Administration grants 50QM0501, 50QM1201, and 50QM1701 to the Christian Albrechts University, Kiel. The data used in this article are available through the NASA Planetary Data System archive, at the Planetary Plasma Interactions node hosted by UCLA, http://pds-ppi.igpp.ucla.edu.

References

Bichsel, H. (1988). Straggling in thin silicon detectors. *Reviews of Modern Physics*, *60*(3), 663–699. https://doi.org/10.1103/RevModPhys.60.663

Blakely, E. A., & Kronenberg, A. (1998). Heavy-ion radiobiology: New approaches to delineate mechanisms underlying enhanced biological effectiveness. *Radiation Research*, *150*(5), S126–S145. https://doi.org/10.2307/3579815

Guo, J., Dumbovic, M., Wimmer-Schweingruber, R. F., Temmer, M., Lohf, H., Wang, Y., et al. (2018). Modeling the evolution and propagation of the 2017 September 9th and 10th CMEs and SEPs arriving at Mars constrained by remote-sensing and in-situ measurement, arXiv:1803.00461v3 [physics.space-ph].

Guo, J., Zeitlin, C., Wimmer-Schweingruber, R. F., Rafkin, S., Hassler, D. M., Posner, A., et al. (2015). Modeling the variations of dose rate measured by RAD during the first MSL Martian year: 2012–2014. *The Astrophysical Journal*, *810*(1), 24–33. https://doi.org/10.1088/0004-637X/810/1/24

Hassler, D. M., Zeitlin, C., Wimmer-Schweingruber, R. F., Boettcher, S., Martin, C., Andrews, J., et al. (2012). The Radiation Assessment Detector (RAD) investigation. *Space Science Reviews*, *170*(1–4), 503–558. https://doi.org/10.1007/s11214-012-9913-1

Hassler, D. M., Zeitlin, C., Wimmer-Schweingruber, R. F., Ehresmann, B., Rafkin, S., Eigenbrode, J. L., et al. (2014). Mars' surface radiation environment measured with the Mars Science Laboratory's Curiosity rover. *Science*, *343*(6169), 1244797. https://doi.org/10.1126/science.1244797

International Commission on Radiation Protection (1991). Publication 60, *Ann. ICRP*, 21 (1–3). Elsevier, Amsterdam.

Köhler, J., Zeitlin, C., Ehresmann, B., Wimmer-Schweingruber, R. F., Hassler, D. M., Reitz, G., et al. (2014). Measurements of the neutron spectrum on the Martian surface with MSL/RAD. *Journal of Geophysical Research: Planets*, *119*, 594–603. https://doi.org/10.1002/2013JE004539

National Council on Radiation Protection and Measurements (1989). Report no. 98, Guidance on Radiation Received in Space Activities. Bethesda, Md.

National Council on Radiation Protection and Measurements (2002). Report no. 142, Operational Radiation Safety Program for Astronauts in Low-Earth Orbit: A Basic Framework. Bethesda, Md.

Onsager, T., Grubb, R., Kunches, J., Matheson, L., Speich, D., Zwickl, R. W., & Sauer, H. (1996). Operational uses of the GOES energetic particle detectors, Proc. SPIE 2812, GOES-8 and Beyond. https://doi.org/10.1117/12.254075

Patrignani, C., & Particle Data Group (2016). Review of particle physics. *Chinese Physics C*, *40*(10), 100,001. https://doi.org/10.1088/1674-1137/40/10/100001

Rossi, H. H. (1964). Correlation of radiation quality and biological effect. *Annals of the New York Academy of Sciences*, *114*(1), 4–15. https://doi.org/10.1111/j.1749-6632.1964.tb53559.x

Zeitlin, C., Hassler, D. M., Cucinotta, F. A., Ehresmann, B., Wimmer-Schweingruber, R. F., Brinza, D. E., et al. (2013). Measurements of energetic particle radiation in transit to Mars on the Mars Science Laboratory. *Science*, *340*(6136), 1080–1084. https://doi.org/10.1126/science.1235989

Zeitlin, C., Hassler, D. M., Wimmer-Schweingruber, R. F., Ehresmann, B., Appel, J., Berger, T., et al. (2016). Calibration and characterization of the radiation assessment detector (rad) on curiosity. *Space Science Reviews*, *201*(1–4), 201–233. https://doi.org/10.1007/s11214-016-0303-y